

IceCube at the Threshold

T. Gaisser¹ for the IceCube Collaboration

Abstract IceCube has observed neutrinos above 100 TeV at a level significantly above the steeply falling background of atmospheric neutrinos. The astrophysical signal is seen both in the high-energy starting event analysis from the whole sky and as a high-energy excess in the signal of neutrino-induced muons from below. No individual neutrino source, either steady or transient, has yet been identified. Several follow-up efforts are currently in place in an effort to find coincidences with sources observed by optical, X-ray and gamma-ray detectors. This paper, presented at the inauguration of HAWC, reviews the main results of IceCube and describes the status of plans to move to near-real time publication of high-energy events by IceCube.

1 Introduction

IceCube, the first kilometer-scale neutrino detector, was completed at the end of 2010 after seven Antarctic seasons. The detector has been in operation since May 2011 with its full complement of 86 strings of digital optical modules (DOMs) in the deep ice and 81 stations of the IceTop array on the surface (see Fig. 1). Somewhat like the relation of HAWC to MILAGRO, the design of IceCube benefitted from its predecessor, AMANDA, as described in the review by A. Karle [1]. In the case of IceCube, the main new feature of the design (apart from the greater size) is the data acquisition system (DAQ) in which waveforms are digitized in each of the 60 DOMs on each string and sent over copper cables to computers in the IceCube Lab for processing. The ability to drill with hot water, deploy optical modules in the deep ice and reconstruct neutrino-induced muons [2] were all demonstrated in AMANDA. The local digitization design of the DAQ was tested on String 18 of AMANDA [3].

Construction of IceCube was supported by the U.S. National Science Foundation with funds from the Major Research Equipment and Facilities Construction Account and by significant additional support from international partners. It is interesting to note that construction of IceCube (which by itself required transport of 4.7 million pounds of equipment to the South Pole) proceeded in parallel with construction of the new South Pole Station and of the South Pole Telescope.

¹Bartol Research Institute and Department of Physics and Astronomy, University of Delaware, Newark, DE 19716

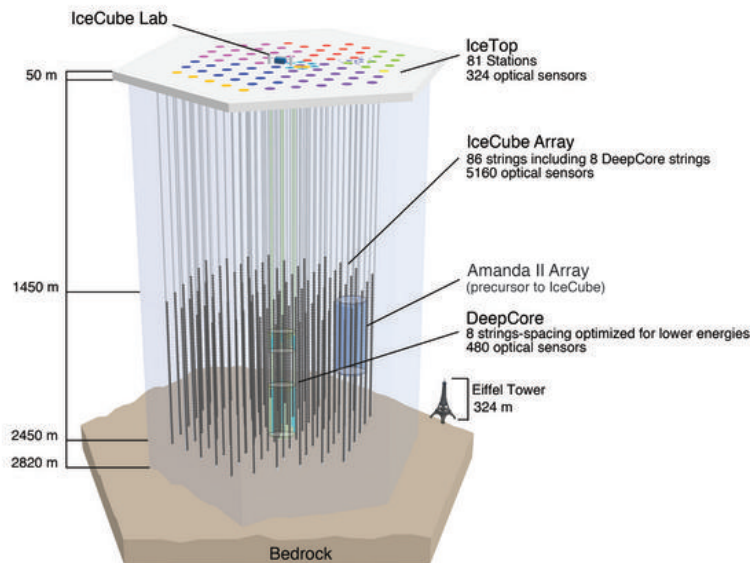


Fig. 1 Artist's view of the IceCube detector.

Analysis of IceCube data began soon after the first string and surface detectors were functioning in 2005-06 [4] and continued with the first study of neutrino-induced upward muons based on data with nine strings in 2006-07 [5]. Studies of neutrino-induced muons continued with increasing sensitivity. They provide the basis of searches for point sources of astrophysical neutrinos [6] as well as a measurement of the spectrum of atmospheric ν_μ [7]. The spectrum of atmospheric electron neutrinos in the TeV range was also measured by making use of cascade-like events [8, 9]. Closely related to the measurement of the flux of atmospheric ν_μ is the search for astrophysical neutrinos, which would show up as a hardening of the spectrum of muon neutrinos at high energy. The measurement of upward ν_μ with data from 2009-10 [10] included a few events with high energy, but not a statistically significant excess.

In 2012 two cascade-like events with \sim PeV in deposited energy that started inside the detector were observed in data taken in 2010-11 (IC 79) and 2011-2012 (IC 86). The events were at the lower boundary of the selection region of a search for much higher energy cosmogenic neutrinos from photo-pion production on the cosmic background radiation [12]. This discovery led to a dedicated search in the same two-year data sample for high energy starting events (HESE). Strong evidence for an excess of astrophysical neutrinos at

high energy above the steeply falling spectrum of atmospheric neutrinos was found in a sample of 28 events that included the two PeV events as well as a mixture of astrophysical neutrinos and background in the 100 TeV range [13]. The discovery of astrophysical neutrinos was confirmed by a continuation of the HESE analysis to a third year of data from 2012-2013 (IC 86-2), which included an event with ~ 2 PeV of deposited energy [14].

The organization of this paper follows the order of the slides presented at Puebla, starting with an overview of the broad scope of IceCube science. Then some details of the HESE analysis and related results are described. This is followed by a section on neutrino point source searches with IceCube and a discussion of implications for what the sources of the astrophysical neutrinos observed by IceCube might be. The paper concludes with a discussion of plans for the future, with emphasis on the plan to make public in near real time information on the highest energy neutrinos.

2 Overview of IceCube Science

Solar flares and supernova search: The first extraterrestrial event seen by IceCube was the ground level cosmic-ray event caused by the solar flare of December 13, 2006 [15]. The event was seen as a sharp increase in the counting rate of the 32 tanks of IceTop in operation at the time, as shown in Fig. 2(left).

Scalar rates of all DOMs in the deep detector are continuously monitored to look for nearby supernovae [16]. The supernova signal would be caused by light generated by interactions of ~ 10 MeV neutrinos within a few meters of individual DOMs.

Cosmic-ray physics with IceCube: The IceTop air shower array consists of 81 stations, each with two tanks separated by 10 m, with a spacing of approximately 125 m between stations [17]. Each tank contains one DOM operating at high gain and one at low gain. The IceTop DOMs are fully integrated into the IceCube DAQ so that cosmic ray events seen in coincidence by IceTop and the deep array of IceCube can be identified and reconstructed. The all-particle spectrum measured with 73 stations of IceTop alone with data taken in 2010-2011 is shown in the right panel of Fig. 2 [18]. The conversion from the measured shower size parameter to primary energy depends on primary composition. The measurement resolves significant structure in the spectrum, as indicated by the power-law fits shown in limited energy ranges.

It is also possible to select events seen in coincidence by IceTop and by the deep array of IceCube as described in [19, 20]. The ratio of signal from the muon bundle in the deep ice to the signal for the shower at the surface is sensitive to the composition of the primary cosmic rays. The analysis uses

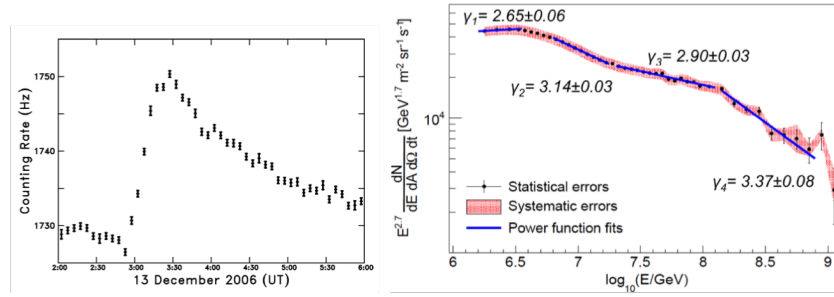


Fig. 2 Left: Ground level solar flare event of December 13, 2006 as seen in the 32 high-gain IceTop DOMs then in operation. Right: cosmic-ray spectrum from IceTop [18] with power-law fits in four segments of the energy range.

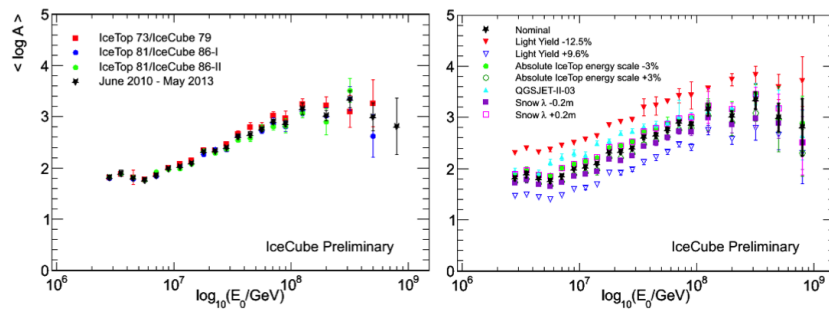


Fig. 3 Mean log of primary mass derived from three years of coincident events (left, with statistical errors only; right, with systematic uncertainties).

a neural network with primary energy and primary mass as fitted variables. An analysis is nearing completion on three years of coincident data consisting of air showers well-reconstructed both in IceTop and in the deep array of IceCube. The preliminary result is shown as a plot of the mean value of the natural logarithm of primary mass in Fig. 3. The energy spectrum obtained from this independent analysis (which makes no a priori assumption about the primary mass composition) confirms the IceTop only measurement (which does require an assumption about energy-dependence of the composition).

A related analysis uses events reconstructed in IceTop with trajectories pointing at the deep array of IceCube but with no muon hits in the deep detector. Such muon poor events can be used to place upper limits on PeV gamma rays from a region of the Galactic plane at high negative declination. An initial search based on data with half the detector has been published [21].

Cosmic-ray anisotropy with IceCube: The event rate in IceCube is dominated by atmospheric muons from above with sufficient energy to penetrate to the detector ($> \approx 500$ GeV). The rate in the full detector is about 3 kHz, with a $\pm 15\%$ seasonal variation. First pass directions and energies are as-

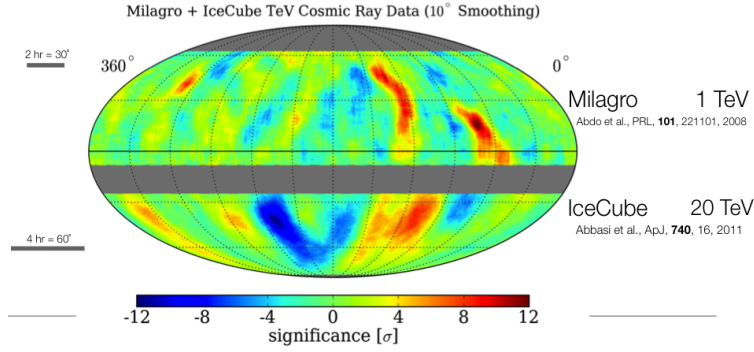


Fig. 4 Significance maps of cosmic-ray anisotropy measured by MILAGRO and IceCube.

signed in the processing and filtering computers at the Pole. These events have been used to measure the cosmic-ray anisotropy in the Southern sky for declinations $< -25^\circ$ [22]. A comparison with Northern hemisphere measurements by MILAGRO [23] is shown in Fig. 4. A joint analysis between IceCube and HAWC will make a single map of the whole sky.

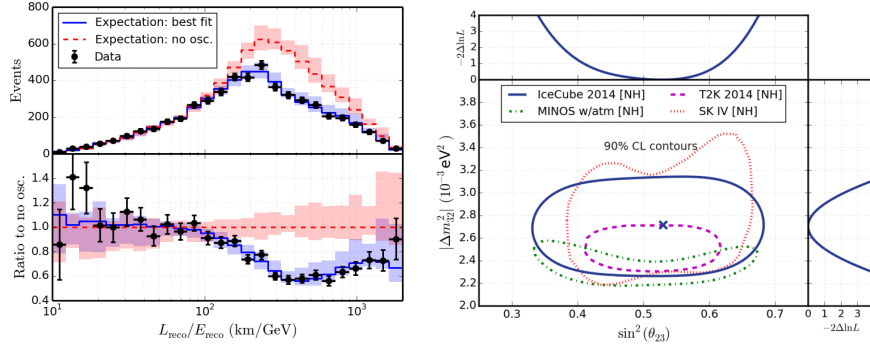


Fig. 5 Left: Ratio (L/E) of path length through the Earth to neutrino energy for atmospheric ν_μ in IceCube. Right: Ninety % confidence level contours for atmospheric neutrino oscillation parameters from the IceCube analysis IceCube Collaboration [24].

Neutrino oscillations: The closely spaced detectors of the DeepCore sub-array of IceCube are used to select a highly pure sample of low energy ν_μ (6 - 56 GeV) from below that produce upward moving muons inside the detector. Selection criteria are designed to ensure that the starting vertex and the decay point of each event are measured well. The neutrino energy is then the sum of the energy of the hadronic shower at the starting vertex and the muon range multiplied by 0.226 GeV/m. Fits to the data are made with the physics quantities $\sin^2 \theta_{23}$ and Δm_{32}^2 as free parameters. The result is shown

in Fig. 5 [24]. A novel feature of this measurement is that the energy range is dominated by the first oscillation minimum in the survival probability, $P_{\nu_\mu\nu_\mu}$ ($E_\nu \approx 25$ GeV).

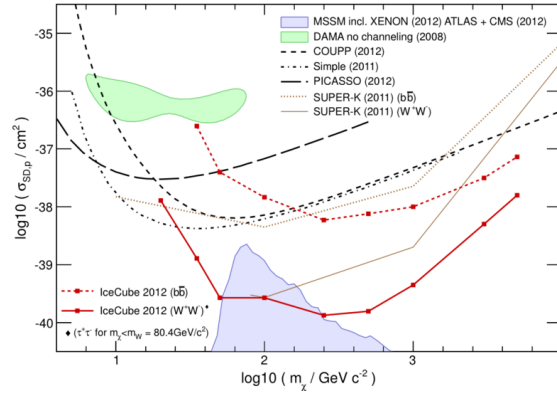


Fig. 6 Upper limit on the WIMP-nucleon spin-dependent cross section based on a search for neutrinos from the Sun by IceCube collaboration [25].

Search for dark matter: There are several approaches to looking for neutrinos from dark matter in IceCube. The most sensitive is the upper limit from annihilation of weakly interacting massive particles (WIMPs) after capture and concentration in the center of the Sun [25]. In equilibrium, the annihilation rate of WIMPs is equal to their capture rate. Thus a limit on neutrinos from WIMP annihilation in the Sun is equivalent to a limit on the capture cross section. Because capture of WIMPs in the Sun is due largely to their interactions with hydrogen, the most significant limit is on the cross section for spin-dependent interactions of WIMPs with nucleons, which is shown in Fig. 6.

3 Astrophysical neutrinos

The key aspect of the HESE analysis is the criterion for selecting events that start inside a fiducial volume surrounded by a veto region and deposit a large amount of light in the detector. This strategy has three key features.

1. The analysis includes events from the whole sky.
2. The background of atmospheric muons that pass the veto and start inside the fiducial volume can be determined from the data by studying muons tagged in the veto region and observing how often they pass a suitably defined inner veto.

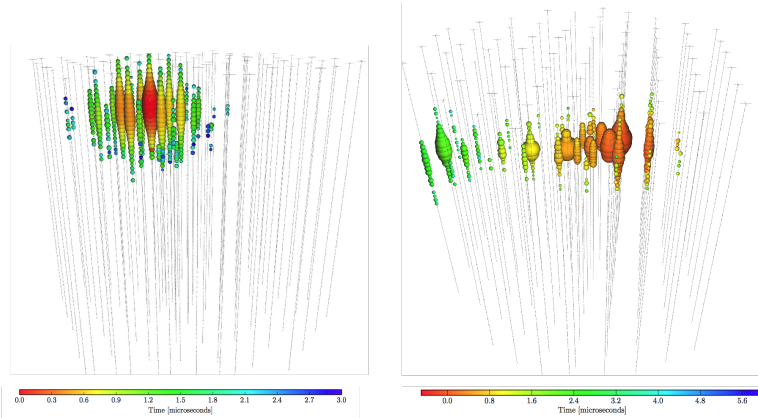


Fig. 7 Left: Cascade event #35 (2 PeV deposited energy); Right: Starting track event #5 (70 TeV deposited energy). Color code: red, early; green/blue late.

3. Atmospheric neutrinos with sufficient energy so that a muon produced in the same air shower would enter the detector are excluded from the event sample.¹

Two events from the high energy starting event analysis are shown in Fig. 7. On the left is the highest energy neutrino observed, a cascade event with deposited energy of 2 PeV, most likely from the charged current interaction of a ν_e . The track event on the right starts inside the detector, deposits an estimated 70 TeV then leaves the detector.

The veto region is shown in Fig. 8 left along with the distribution in energy of events for data from three years. The excess, which has a significance of 5.7σ [14], is attributed to high-energy neutrinos of astrophysical origin. Assuming a differential spectral index of -2 for the astrophysical component and a flavor ratio at Earth of $1 : 1 : 1$, the astrophysical flux per flavor ($\nu + \bar{\nu}$) is

$$E^2 \phi(E) = 0.95 \pm 0.3 \times 10^{-8} \text{ GeV s}^{-1} \text{ sr}^{-1} \text{ cm}^{-2}. \quad (1)$$

A fit to the astrophysical component without a prior constraint on its spectral index allows spectral indexes from -2.0 to -2.3 depending on the background of prompt neutrinos. The best fit is at the lower boundary of the interval at

$$E^2 \phi(E) = 1.5 \times 10^{-8} \left(\frac{E}{100 \text{ TeV}} \right)^{-0.3} \text{ GeV s}^{-1} \text{ sr}^{-1} \text{ cm}^{-2}. \quad (2)$$

¹ There are two cases of the atmospheric neutrino self-veto: when the vetoing muon is from the same decay in which the neutrino was produced [26]; and a generalized veto that includes any muon produced in the same air shower [27]. The latter is needed in particular for electron neutrinos where the accompanying lepton at production is an electron or positron.

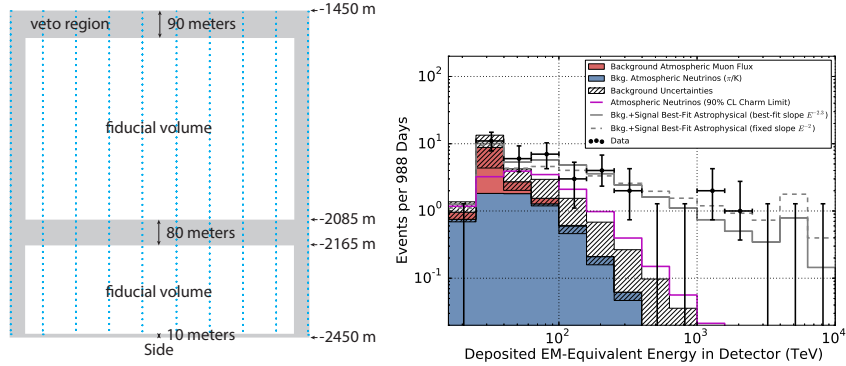


Fig. 8 Left: Veto region for HESE analysis; Right: Energy distribution of events in the 3-year HESE analysis [14].

If the flavor ratio of anti-neutrinos at Earth is $(\bar{\nu}_e : \bar{\nu}_\mu : \bar{\nu}_\tau) = (1 : 1 : 1)$, the harder spectrum (Eq. 1) cannot continue unbroken above the threshold of 6.3 PeV for the Glashow process, $\bar{\nu}_e + e^- \rightarrow W^-$. Three events with energies above 2 PeV would have been expected for an unbroken E^{-2} spectrum [14].

A subsequent analysis extends the HESE selection strategy to lower energy by defining a set of nested, increasingly smaller fiducial volumes [28]. The analysis covers 641 days, overlapping the two-year HESE analysis [13]. The lowest threshold corresponds to approximately 1 TeV of deposited energy in the detector. The analysis finds 105 track events and 283 cascade events, including the two 1 PeV events seen in the two-year HESE analysis [13].² The analysis makes use of the different characteristic energy and angular dependences of conventional atmospheric neutrinos, prompt atmospheric neutrinos, muon background and astrophysical neutrinos to fit the components separately. An upper limit of 1.5 times the prediction of Enberg et al. [29] at 90% confidence level is set on the charm contribution. The astrophysical component is fit with a relatively soft spectrum,

$$E^2\phi(E) = 2.06_{-0.26}^{+0.35} \times 10^{-8} \left(\frac{E}{100 \text{ TeV}} \right)^{-0.46 \pm 0.12} \text{ GeV s}^{-1} \text{ sr}^{-1} \text{ cm}^{-2}. \quad (3)$$

It is pointed out that such a soft spectrum of neutrinos, if produced by proton-proton collisions in optically thin regions, would lead to $\pi^0 \rightarrow \gamma\gamma$ production at a level greater than allowed by the diffuse gamma-ray background observed by Fermi-LAT [32]. (See Murase et al. [33]).

² It is important to keep in mind that the fixed threshold on deposited energy biases against track events from charged current interactions of ν_μ because a significant fraction of the neutrino energy leaves the detector. Two recent analyses [30, 31] shows that the flavor ratios of the astrophysical neutrinos in IceCube are consistent with the 1 : 1 : 1 ratio expected at Earth after oscillations over astrophysical distances.

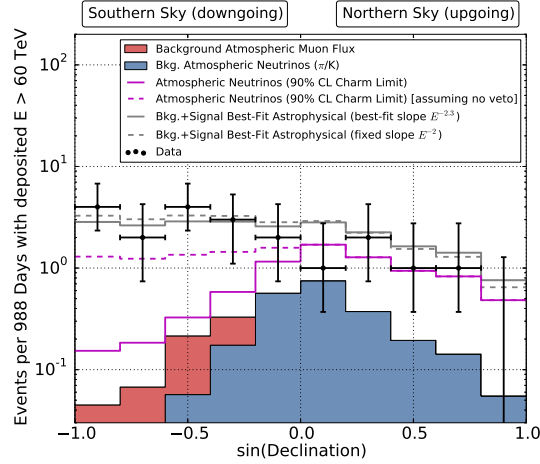


Fig. 9 Angular distribution of events with deposited energy > 60 TeV in the HESE 3-year analysis [14]. The solid pink histogram shows the 90% c.l. upper limit from prompt neutrinos. See text for discussion.

The prompt component of atmospheric neutrinos will have a spectral index ≈ -2.7 , similar to that of the primary spectrum of nucleons in the energy range of tens of TeV, approximately one power harder than conventional atmospheric neutrinos from decay of kaons and pions. It is therefore important to understand the low limits on the prompt contribution to the background found in IceCube starting event analyses. A feature of the atmospheric neutrino self-veto is relevant in this context, as illustrated in Fig. 9. The solid pink histogram shows the shape of angular distribution of prompt neutrinos from decay of charm in the HESE analysis. The broken pink histogram shows the prompt contribution in the absence of the self-veto. For neutrino energies below about 10 PeV, neutrinos from decay of charmed hadrons are produced isotropically in the atmosphere. In the absence of the neutrino self-veto, the expected flux would be nearly isotropic apart from the suppression for nearly upward events due to absorption in the Earth. Instead, the neutrino self-veto suppresses the downward contribution significantly. The absence of a contribution with this shape contributes to the low upper limit on charm from this [28] analysis.

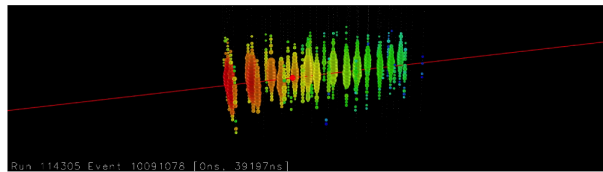


Fig. 10 High-energy ν_μ -induced muon crossing IceCube from below the horizon [10].

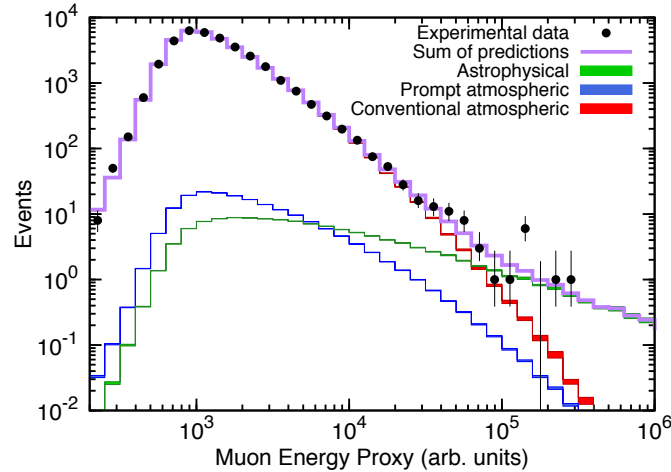


Fig. 11 Energy spectrum of ν_μ -induced muons measured from 2010-2012 [11].

Figure 10 shows a neutrino-induced muon entering IceCube from below the horizon in the analysis of data taken in 2009-2010 [10]. With analysis of two more years of data (2010-2012) with the larger detector, the astrophysical signal is becoming visible also in this channel at a level above 3σ [11]. The observed energy spectrum and fits of atmospheric and astrophysical neutrino-induced muons are shown in Fig. 11. The best fit parent astrophysical neutrino spectrum is

$$E^2\phi(E) = 1.7_{-0.8}^{+0.6} \times 10^{-8} \left(\frac{E}{100 \text{ TeV}} \right)^{-0.2 \pm 0.2} \text{ GeV s}^{-1} \text{ sr}^{-1} \text{ cm}^{-2}. \quad (4)$$

4 Search for point sources

Neutrino-induced muons provide the best sensitivity for point sources because the muon tracks provide good angular resolution ($< 1^\circ$) and the rates are higher for a given flux because of the larger effective target volume achieved by accepting muons that start outside the instrumented volume. The most recently published search for steady sources [6] covers four years, 2008-09 (IC40), 2009-10 (IC59), 2010-2011 (IC79) and 2011-12 (IC86). No significant concentration of events is found.

In addition to the all-sky scan, the analysis also looks at a selected list of 44 likely sources, 14 galactic and 30 extragalactic. Upper limits for this search are shown in Fig. 12 along with upper limits from ANTARES [34]. The IceCube sensitivities and limits are shown in this plot assuming E^{-2}

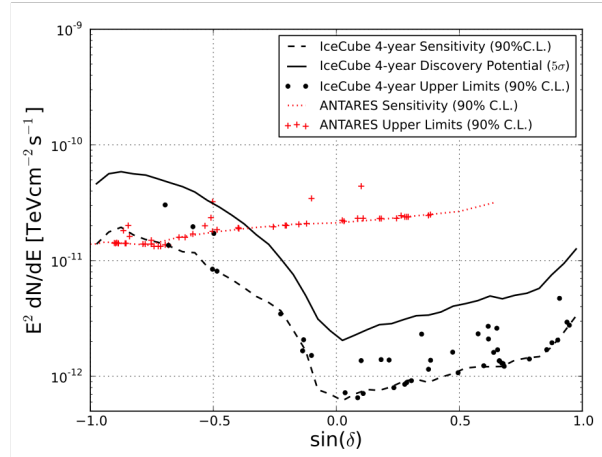


Fig. 12 Upper limits on neutrinos from selected point sources from IceCube (black) and ANTARES (red). (Figure from IceCube Collaboration [6].)

differential spectra. In the Northern sky, typical limits are at the level

$$E^2 \frac{dN}{dE} \approx 2 \times 10^{-9} \text{ GeV cm}^{-2} \text{ s}^{-1}. \quad (5)$$

In order to include the Southern sky, which is dominated by a high flux of atmospheric muons at the South Pole, the energy threshold is set very high in IceCube to reduce the background.³ ANTARES has good sensitivity down to lower energy. A joint analysis between ANTARES and IceCube is underway. In addition, two more years of data (2012-14) with the full IceCube will soon be added to the search for steady sources.

It is also of course possible to search for transient source of neutrinos, such as AGN flares and gamma-ray bursts (GRBs). Searches for events clustered in time as well as events from particular sources known to flare have so far not found any significant correlation [35]. Particularly significant limits come from the absence of neutrinos associated with GRBs [36, 37]. The most recent IceCube search for neutrinos in association with GRB is inconsistent with standard models of optically thin gamma-ray bursts [37]. The analysis finds that no more than $\sim 1\%$ of the HESE flux consists of prompt emission from GRBs potentially observable by exiting satellites.

The high-energy events from the HESE analysis are distributed over the sky, with some near the galactic plane (including a statistically insignificant cluster near the galactic center), but with many far away from the plane. (See Fig. 13.) The angular resolution for the cascade events is $\sim 15^\circ$, so there are many potential sources within the cone defined by each event. Padovani

³ The small improvement in IceCube sensitivity for declinations near -90° is achieved by using IceTop as a veto.

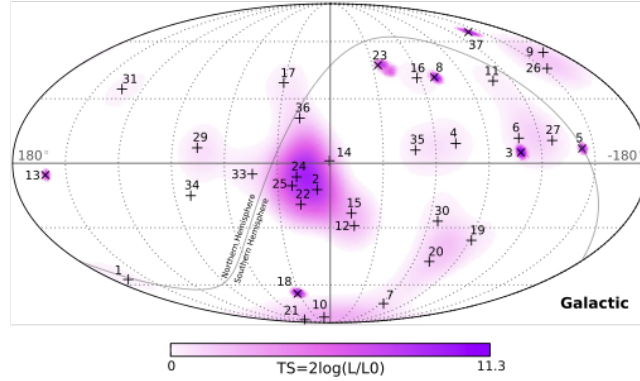


Fig. 13 Map in galactic coordinates of the events from the three-year HESE analysis [14].

& Resconi [38] show that it is nevertheless possible to use the energetics of sources such as blazars and pulsar wind nebulae to select candidate sources within the error circles of many of the events with sufficient power to be the corresponding sources.

Many, if not all, of the astrophysical events in the HESE sample are most likely of extragalactic origin. Ahlers & Halzen [39] show that, in this case, it is possible to use the observed luminosity density of the HESE flux (e.g. from Eq. 1) together with the upper limits from the point source search (Eq. 5) to constrain the classes of sources responsible for the astrophysical neutrino flux in IceCube. The argument is basically geometric, comparing the integral over the neutrinos from all sources in the Universe with the flux from a typical nearby source [40]. Transient sources are constrained in a similar way. For steady sources the luminosity density is

$$L\rho = \frac{\text{energy}}{\text{source} \cdot \text{time}} \times \frac{\text{sources}}{\text{volume}}, \quad (6)$$

while for transient sources (here < 100 s) it is

$$L\rho = \frac{\text{energy}}{\text{burst}} \times \frac{\text{bursts}}{\text{volume} \cdot \text{time}}. \quad (7)$$

Figure 14 by Kowalski [41] displays the present IceCube constraints on various source classes on a single diagram. The diagonal line is obtained by equating the observed flux from all flavors ($3 \times \text{Eq. 1}$) to the integral of the neutrino flux from the Universe. The result is

$$\xi \frac{L_\nu \rho R_H}{4\pi} = \frac{E_\nu^2 dN_\nu}{d\Omega dE_\nu} \approx 2.8 \times 10^{-8} \frac{\text{GeV}}{\text{cm}^2 \text{sr s}}, \quad (8)$$

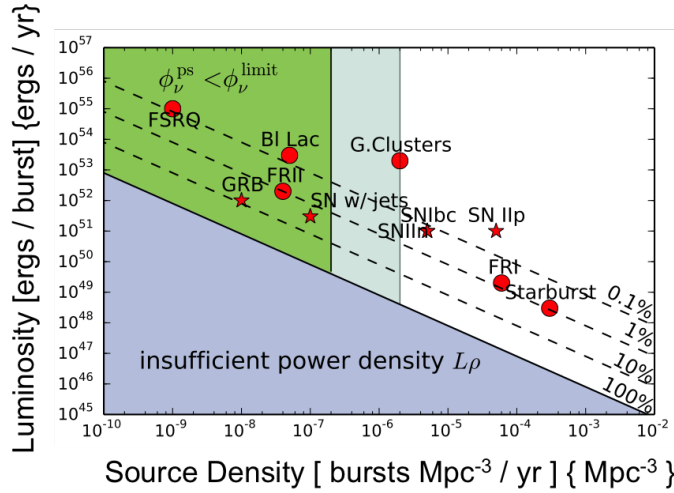


Fig. 14 Diagram with limits on the contribution of various source classes to IceCube’s astrophysical neutrino flux [41]. Axis labels are in different brackets for [transient] and {steady} sources.

where R_H is the Hubble radius and ξ is a cosmological factor of order 3 which depends on the cosmological evolution of the particular class of sources. This gives $L\rho \sim 10^{43}$ erg/Mpc³/yr, which is the diagonal line in the diagram. A class of sources must have a value of luminosity density greater than this to account for the observed flux. The vertical lines represent the minimum density of sources (left line for steady sources) or rate density (right line for transient sources) allowed by the non-observation of the various source classes. For example, equating the typical steady point source limit from Eq. 5 to the flux $L/(4\pi d_1^2)$ with $d_1 = (4\pi\rho)^{-1/3}$ gives a minimum density of $\sim 10^{-7}$ Mpc⁻³.

5 Plans for the future

IceCube is currently in the position of having discovered high-energy astrophysical neutrinos without yet establishing what the sources are. Upper limits are placing significant constraints on particular classes of potential sources. For example, although blazars are attractive candidates [38], an analysis of the Fermi-LAT catalog of blazars [42] concludes that the sources in that catalog cannot count for more than about 20% of the observed astrophysical flux. Starburst galaxies [43] are an attractive potential class of sources, in part because of their relatively low luminosity and relatively high density. On the other hand, depending on how steeply the astrophysical spectrum extends to low energy [44], they may be in conflict with Fermi observations of the diffuse gamma-ray background [45].

5.1 Short term

In this situation it is important to exploit multi-wavelength and multi-messenger opportunities as much as possible by making neutrino data available to other observers as quickly as possible. There are ongoing analyses looking for correlations of HESE events with existing catalogs of bright transients, but the sensitivity of such an analysis is determined by the threshold set in making the catalog. Triggering followup observations with IceCube neutrinos instead can significantly improve the chance of finding coincidences. IceCube currently sends alerts under agreements with various other observatories. For example, the optical/X-ray follow-up (OFU/XFU) program sends alerts to the Palomar Transient Facility and to SWIFT whenever two neutrino-induced muons occur within a 100 seconds of each other a point to the same direction within 3.5° . The gamma follow-up (GFU) monitors selected sources and sends alerts to MAGIC and VERITAS.

The OFU/XFU/GFU follow-up data stream has recently been augmented to include single neutrinos of interest, which are being sent north at a rate of 5 mHz. Events from the Southern hemisphere are now included with criteria suitable for selecting likely neutrino candidates, and H.E.S.S. is added to the list of receiving observatories. The single event stream will be used to send events to the Astrophysical Multimessenger Observatory Network (AMON) [46] for sharing of sub-threshold data among multi-messenger observatories.

For HESE events, a starting event filter has been implemented that will provide alerts in real time. A short message with information from the online filter, including a probability of track vs. cascade, will be sent to AMON. The treatment of the starting events will depend on their brightness. GCN alerts will be generated for events with more than 6000 p.e. (~ 30 TeV and 10-15/year). Starting events with more than 1500 but less than 6000 p.e. (≈ 4 /day) will be included in the AMON sub-threshold data sharing scheme. Upgrades to the satellite connection from the South Pole will allow full event information to be sent with delays of order one minute. This will provide the basis for full reconstruction of events. Alerts can be revised accordingly for the brightest events.

5.2 Long term

For the longer term future, plans for expanding IceCube to collect more high energy neutrinos are underway [47]. Figure 15 is a picture of what such an expanded array might look like. IceCube Gen2 includes the Precision IceCube Next Generation Upgrade (PINGU) [48] for precision studies of neutrino physics, including mass hierarchy.

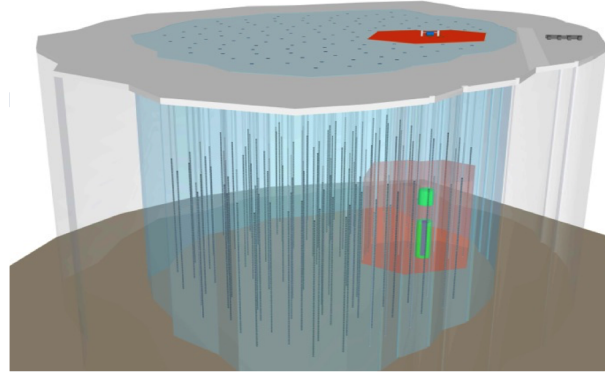


Fig. 15 Concept for an expanded version of IceCube [47]. PINGU is indicated by the dense shading inside DeepCore.

Acknowledgements I thank the HAWC Collaboration for the opportunity to bring congratulations from IceCube on the occasion of the inauguration of HAWC. I am grateful to Erik Blaufuss and Marek Kowalski for help preparing this paper, and I thank my colleagues in IceCube for the science summarized in this paper. It is a pleasure to acknowledge the National Science Foundation for their support of IceCube and of my own research. A full list of agencies supporting IceCube is posted at <http://icecube.wisc.edu/Collaboration/funding>. The list of IceCube institutions is available at <http://icecube.wisc.edu/collaboration>.

References

- [1] Karle, A., “The Path from AMANDA to IceCube,” in Proc. IAU Symposium 288 (Cambridge University Press, 2012)
- [2] AMANDA Collaboration, Abbasi, R., Ackermann, M., Adams, J., et al. 2009, “Search for Point Sources of High Energy Neutrinos with Final Data from AMANDA-II,” *Physical Review D*, 79, 062001
- [3] AMANDA Collaboration, Ahrens, J., Bai, X., et al. 2006, “The ICECUBE prototype string in AMANDA,” *Nuclear Instruments and Methods in Physics Research A*, 556, 169
- [4] IceCube Collaboration, Achterberg, A., Ackermann, M., et al. 2006, “First Year Performance of The IceCube Neutrino Telescope,” *Astroparticle Physics*, 26, 155
- [5] IceCube Collaboration, Achterberg, A., Ackermann, M., Adams, J., et al. 2007, “Detection of Atmospheric Muon Neutrinos with the IceCube 9-String Detector,” *Physical Review D*, 76, 027101
- [6] IceCube Collaboration, Aartsen, M. G., Ackermann, M., et al. 2014, “Searches for Extended and Point-like Neutrino Sources with Four Years of IceCube Data,” *Astrophys. J.*, 796, 109
- [7] IceCube Collaboration, Abbasi, R., Abdou, Y., Abu-Zayyad, T., et al. 2011, “Measurement of the atmospheric neutrino energy spectrum from 100 GeV to 400 TeV with IceCube,” *Physical Review D*, 83, 012001

- [8] IceCube Collaboration, Aartsen, M. G., Abbasi, R., Abdou, Y., et al. 2013, "Measurement of the Atmospheric ν_e flux in IceCube," *Physical Review Letters*, 110, 151105
- [9] IceCube Collaboration, Aartsen, M. G., Ackermann, M., et al. 2015, "Measurement of the Atmospheric ν_e Spectrum with IceCube," *Physical Review D*, 91, 122004
- [10] IceCube Collaboration, Aartsen, M. G., Abbasi, R., et al. 2013, "Search for a diffuse flux of astrophysical muon neutrinos with the IceCube 59-string configuration," *Physical Review D*, 89, 062007
- [11] IceCube Collaboration, Aartsen, M. G., Abraham, K., et al. 2015, "Evidence for Astrophysical Muon Neutrinos from the Northern Sky with IceCube," arXiv:1507.04005, accepted for *Phys. Rev. Letters*
- [12] IceCube Collaboration, Aartsen, M. G., Abbasi, R., Abdou, Y., et al. 2013, "First observation of PeV-energy neutrinos with IceCube," *Physical Review Letters*, 111, 021103
- [13] IceCube Collaboration, Aartsen, M. G., Abbasi, R., Abdou, Y. et al. 2013, "Evidence for High-Energy Extraterrestrial Neutrinos at the IceCube Detector," *Science*, 342, 1242856
- [14] IceCube Collaboration, Aartsen, M. G., Ackermann, M., Adams, J., et al. 2014, "Observation of High-Energy Astrophysical Neutrinos in Three Years of IceCube Data," *Physical Review Letters*, 113, 101101
- [15] IceCube Collaboration, Abbasi, R., Ackermann, M., Adams, J., et al. 2008, "Solar Energetic Particle Spectrum on 13 December 2006 Determined by IceTop," *Astrophysical Journal Letters*, 689, L65
- [16] IceCube Collaboration, Abbasi, R., Abdou, Y., et al. 2011, "IceCube Sensitivity for Low-Energy Neutrinos from Nearby Supernovae," *Astron. Astrophys.* 535, A109
- [17] IceCube Collaboration, Abbasi, R., Abdou, Y., Ackermann, M., et al. 2013, "IceTop: The surface component of IceCube," *Nuclear Instruments and Methods in Physics Research A*, 700, 188
- [18] IceCube collaboration, Aartsen, M. G., Abbasi, R., Abdou, Y. et al. 2013, "Measurement of the cosmic ray energy spectrum with IceTop-73," *Physical Review D*, 042004
- [19] IceCube Collaboration, Abbasi, R., Abdou, Y., et al. 2013, "Cosmic Ray Composition and Energy Spectrum from 1-30 PeV Using the 40-String Configuration of IceTop and IceCube," *Astroparticle Physics*, 42, 15
- [20] IceCube Collaboration, Aartsen, M. G., Abbasi, R., et al. 2013, "The IceCube Neutrino Observatory Part III: Cosmic Rays," arXiv:1309.7006
- [21] Aartsen, M. G., Abbasi, R., Abdou, Y., et al. 2013, "Search for Galactic PeV Gamma Rays with the IceCube Neutrino Observatory," *Physical Review D*, 87, 062002
- [22] IceCube Collaboration, Abbasi, R., Abdou, Y., Abu-Zayyad, T., et al. 2011, "Observation of Anisotropy in the Arrival Directions of Galactic Cosmic Rays at Multiple Angular Scales with IceCube," *Astrophys. J.*, 740, 16

- [23] Abdo, A. A., Allen, B., Aune, T., et al. 2008, “Discovery of Localized Regions of Excess 10-TeV Cosmic Rays,” *Physical Review Letters*, 101, 221101
- [24] IceCube Collaboration, Aartsen, M. G., Ackermann, M., et al. 2015, “Determining neutrino oscillation parameters from atmospheric muon neutrino disappearance with three years of IceCube DeepCore data,” *Physical Review D*, 91, 072004
- [25] IceCube collaboration, Aartsen, M. G., Abbasi, R., et al. 2012, “Search for dark matter annihilations in the Sun with the 79-string IceCube detector,” arXiv:1212.4097
- [26] Schönert, S., Gaisser, T. K., Resconi, E., & Schulz, O. 2009, “Vetoing atmospheric neutrinos in a high energy neutrino telescope,” *Physical Review D*, 79, 043009
- [27] Gaisser, T. K., Jero, K., Karle, A., & van Santen, J. 2014, “Generalized self-veto probability for atmospheric neutrinos,” *Physical Review D*, 90, 023009
- [28] IceCube Collaboration, Aartsen, M. G., Ackermann, M., Adams, J., et al. 2015, “Atmospheric and astrophysical neutrinos above 1 TeV interacting in IceCube,” *Physical Review D*, 91, 022001
- [29] Enberg, R., Reno, M. H., & Sarcevic, I. 2008, “Prompt neutrino fluxes from atmospheric charm,” *Physical Review D*, 78, 043005
- [30] IceCube Collaboration, Aartsen, M. G., Ackermann, M., Adams, J., et al. 2015, “Flavor Ratio of Astrophysical Neutrinos above 35 TeV in IceCube,” *Physical Review Letters*, 114, 171102
- [31] IceCube Collaboration, Aartsen, M. G., Abraham, K., et al. 2015, “A combined maximum-likelihood analysis of the high-energy astrophysical neutrino flux measured with IceCube,” arXiv:1507.03991
- [32] Fermi LAT Collaboration, Abdo, A. A., Ackermann, M., Ajello, M., et al. 2010, “The Spectrum of the Isotropic Diffuse Gamma-Ray Emission Derived From First-Year Fermi Large Area Telescope Data,” *Physical Review Letters*, 104, 101101
- [33] Murase, K., Ahlers, M., & Lacki, B. C. 2013, “Testing the Hadronuclear Origin of PeV Neutrinos Observed with IceCube,” *Physical Review D*, 88, 121301
- [34] Adrián-Martínez, S., Samarai, I. A., Albert, A., et al. 2012, “Search for Cosmic Neutrino Point Sources with Four Year Data of the ANTARES Telescope,” *Astrophys. J.*, 760, 53
- [35] IceCube Collaboration, Aartsen, M. G., Ackermann, M., Adams, J., et al. 2015, “Searches for Time Dependent Neutrino Sources with IceCube Data from 2008 to 2012,” *Astrophys. J.*, 807, 46
- [36] IceCube Collaboration, Abbasi, R., Abdou, Y., Abu-Zayyad, T., et al. 2012, “An absence of neutrinos associated with cosmic-ray acceleration in γ -ray bursts,” *Nature*, 484, 351

- [37] IceCube Collaboration, Aartsen, M. G., Ackermann, M., et al. 2015, “Search for Prompt Neutrino Emission from Gamma-Ray Bursts with IceCube,” *Astrophys. J.*, 805, L5
- [38] Padovani, P., & Resconi, E. 2014, “Are both BL Lacs and pulsar wind nebulae the astrophysical counterparts of IceCube neutrino events?,” *Mon. Not. R. Astron. Soc.*, 443, 474
- [39] Ahlers, M., & Halzen, F. 2014, “Pinpointing Extragalactic Neutrino Sources in Light of Recent IceCube Observations,” *Physical Review D*, 90, 043005
- [40] Lipari, P. 2008, “Proton and Neutrino Extragalactic Astronomy,” *Physical Review D*, 78, 083011
- [41] Kowalski, M. 2014, “Status of High-Energy Neutrino Astronomy,” arXiv:1411.4385
- [42] Glüsenkamp, T., for the IceCube Collaboration 2015, “Analysis of the cumulative neutrino flux from Fermi-LAT blazar populations using 3 years of IceCube data,” arXiv:1502.03104
- [43] Loeb, A., & Waxman, E. 2006, “The Cumulative background of high energy neutrinos from starburst galaxies,” *JCAP*, 5, 003
- [44] Senno, N., Mészáros, P., Murase, K., Baerwald, P., & Rees, M. J. 2015, “Extragalactic star-forming galaxies with hypernovae and supernovae as high-energy neutrino and gamma-ray sources: the case of the 10 TeV neutrino data,” arXiv:1501.04934
- [45] The Fermi LAT collaboration, Ackermann, M., Ajello, M., et al. 2015, “The spectrum of isotropic diffuse gamma-ray emission between 100 MeV and 820 GeV,” *Astrophys. J.*, 799, 86
- [46] Smith, M. W. E., Fox, D. B., Cowen, D. F., et al. 2013, “The Astrophysical Multimessenger Observatory Network (AMON),” *Astroparticle Physics*, 45, 56
- [47] IceCube-Gen2 Collaboration, Aartsen, M. G., et al. 2014, “IceCube-Gen2: A Vision for the Future of Neutrino Astronomy in Antarctica,” arXiv:1412.5106
- [48] The IceCube-PINGU Collaboration Aartsen, M. G., et al. 2014, “Letter of Intent: The Precision IceCube Next Generation Upgrade (PINGU),” arXiv:1401.2046